

Temperature dependence of anisotropic stress–rupture properties of nickel-based single crystal superalloy SRR99

HAN Guo-ming, YANG Yan-hong, YU Jin-jiang, SUN Xiao-feng

Institute of Metal Research, Chinese Academy of Sciences, Shenyang 110016, China

Received 18 October 2010; accepted 16 December 2010

Abstract: In order to reveal the temperature dependence of anisotropic stress–rupture behavior of SRR99 single crystal superalloys under conditions of temperature ranging from 650 to 1 040 °C and typical stresses, fracture morphologies and microstructure evolution were investigated by SEM and TEM. From the Larson–Miller curves, it is found that single crystal with [001] orientation has the optimum stress rupture property in comparison with [011] and [111] orientations at lower and intermediate temperature. With increasing temperature to 1 040 °C, stress–rupture properties of single crystals with three principal orientations tend to be equivalent. Based on the fracture surface and microstructural observations, superior stress–rupture behavior of single crystal with [001] orientation was rationalized and the effect of misorientation of single crystal on stress rupture property was also discussed.

Key words: single crystal superalloy; stress–rupture property; anisotropy; deformation mechanism

1 Introduction

During the past 30 years, nickel-based superalloys have developed from polycrystalline, columnar-grained superalloy to single crystal and have been widely used as critical components such as gas turbine blades[1]. Due to the elimination of grain-boundary strengthening elements such as boron and carbon, creep property and fatigue life of superalloys, particularly at higher temperature, have been improved greatly[2]. On the other hand, solid solution strengthening mainly from addition of W, Mo, Ta and etc, and precipitate hardening dependent on γ' particles are also responsible for this superior mechanical strength [3–4]. It is well known that the mechanical properties of single crystal are inherently anisotropic and single crystals are produced using the withdrawal process with a selector technique deviate from accurate $\langle 001 \rangle$ orientation. Moreover, blades with complex air-cooling channels often experience complicated stresses in a variety of orientations owing to local hot spots, bending moments and torsional stresses across the blade under service. Therefore, the anisotropic creep property of single crystal has been investigated extensively [5–8]. MACKAY and MAIER [9] reported that the stress–

rupture lives of MAR-M247 single crystals were strongly dependent on the lattice rotations towards to multiple slip systems to produce intersecting slip and work hardening. They assumed that large rotation resulted in a higher effective stress and a shorter stress rupture life. SASS et al [10] concluded that crystals oriented to the [001]–[011] boundary exhibited superior creep strength in comparison with crystals close to the [001]–[111] boundary at intermediate temperature. However, little information about the temperature and stress dependence of creep property is available to predict the stress–rupture life time of single crystals. The objective of present work is to study the temperature and stress dependence of stress–rupture behavior of single crystal super alloy SRR99 in order to rationalize the difference and similarity of stress–rupture property of three principal orientations [001], [011] and [111]. Fracture features and deformation mechanisms of single crystal superalloys oriented to [001] under typical conditions were observed by SEM and TEM and primarily discussed due to technological relevance.

2 Experimental

The alloy used in the present work was the

monocrystalline nickel-based superalloy SRR99. The nominal chemical composition of this alloy is shown in Table 1. Single crystals with different orientations were produced by directional solidification technique. The crystallographic orientations of single crystals were determined by EBSD method, and samples deviating from principal orientations within 7° were received a standard heat treatment. The heat treatment given to the material consisted of a step solution treatment at 1 300 °C for 4 h, followed by a two-step aging treatment of 1 100 °C for 4 h and 870 °C for 16 h. The stress–rupture tests were performed under conditions of temperature ranging from 650 to 1 040 °C and typical stresses in air.

After the testing, the fracture surfaces of ruptured specimens were observed by SEM. All thin foils for TEM observation were cut parallel to (001) crystallographic planes from specimens oriented close to [001], then mechanically ground to 50 μm and finally electron-polished at -25°C in a solution of 8% perchloric acid + 92% ethanol.

Table 1 Nominal composition of SRR99 alloy (mass fraction, %)

Al	Ti	Cr	Co
5.5	2.2	8.5	5.0
Ta	W	C	Ni
2.8	9.5	0.015	Bal.

3 Results and discussion

3.1 Microstructure

Figure 1 shows the microstructure of [001]-oriented single crystal in the as-cast condition. The dendritic structure of the alloys is evident (Fig. 1(a)) and some blocky carbides are formed in the interdendritic regions (Fig. 1(b)).

Figure 2 shows that cuboidal γ' particles are coherently set in a face centered cubic (FCC) nickel-based solid solution γ -matrix. The volume fraction of γ' is about 75% and an average edge length is approximately 0.45 μm .

3.2 Stress–rupture property

Larson-Miller curves are often used to predict the creep property of superalloys. The Larson-Miller parameter is often described as $P=T(20+\lg t)10^{-3}$, where T is the temperature of creep test and t is the stress rupture lifetime. In this study, the plot of applied stress vs Larson-Miller parameter shown in Fig. 3 gives a series of experimental results at wide temperature and stress ranges. From this plot, it can be seen that the stress–rupture life time of [001] oriented single crystals

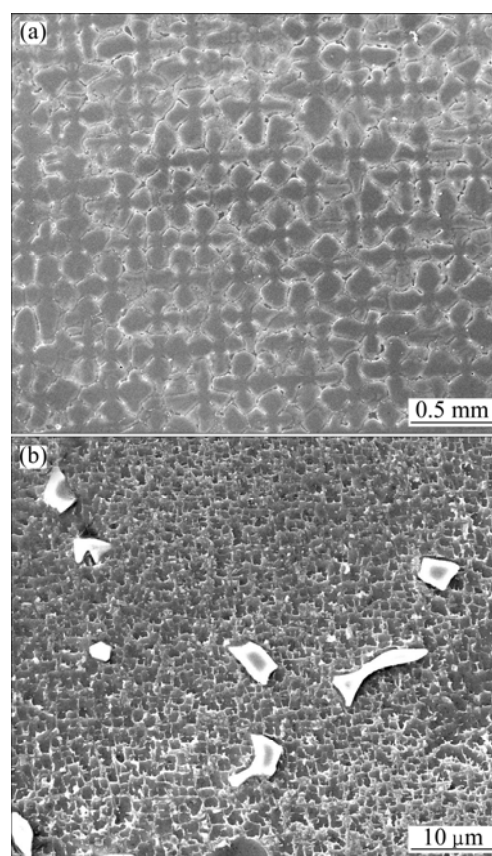


Fig. 1 As-cast microstructure of SRR99 cut along (001) plane showing dendritic morphology (a) and some blocky carbides (b)

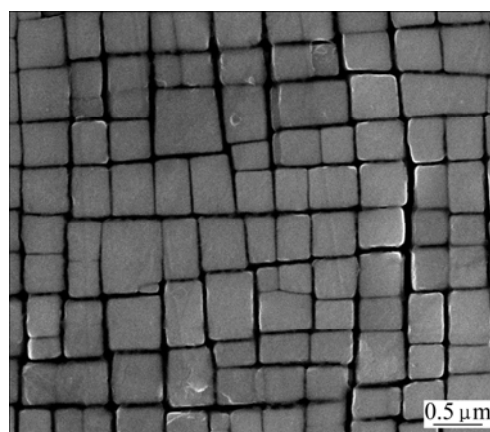


Fig. 2 Cuboidal γ' particles after standard heat treatment of single crystal superalloys SRR99

is significantly longer than that of crystals with [011] or [111] orientation. This tendency is obvious at lower temperature and higher stress. With increasing temperature, the difference of rupture life time among three principal orientations is reduced, which indicates that the anisotropy of stress–rupture decreases with increasing temperature. In addition, the difference of stress–rupture property between single crystals with

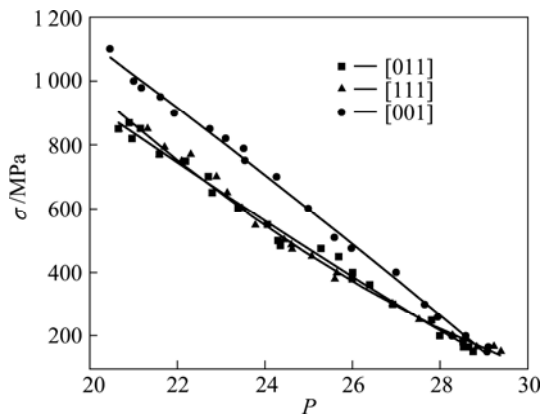


Fig. 3 Comparison of Larson-Miller curves for three principal orientations of SRR99 alloy ($P=T(20+\lg t)10^{-3}$)

[011] and [111] directions is not distinctive in the entire temperature ranges. In order to gain insight into the stress–rupture anisotropic behavior and the effect of temperature on this behavior, a great number of experiments have been done and the results to clarify fracture and deformation mechanisms of three principal orientations have been demonstrated in Ref. [11]. In the present study, attention is greatly paid to the stress–rupture properties of single crystals deviating from [001], and anisotropic behavior is discussed based on $\langle 112 \rangle$ {111} slip system which dominates the creep deformation.

Figure 4 shows some typical fracture surfaces of the [001]-oriented specimens ruptured at intermediate temperature (Fig. 4(a)) and high temperature (Fig. 4(b)). At intermediate temperature, the crack surface is composed of (001) planes, which are perpendicular to the applied stress and denoted as cleavage planes. On (001) planes, there are some cast shrinkage voids which may be the disadvantage for creep property. The differences of fracture surfaces with [011] and [111] compared to that with [001] are that one or two shear planes are inclined to certain angles with stress axis. The main reason for this is the number of octahedral slip systems activated for different single crystals. Therefore, a greater number of slip systems is favorable to form a flat and smooth plane normal to stress axis during the deformation process. With increasing temperature, small internal voids combine and grow into large cavities with the aid of element diffusion (Fig. 4(b)). Fracture surfaces of three principal orientations exhibit the same fracture behavior, which indicates that the deformation under higher temperature is similar to that discussed below.

Representative dislocation configurations at intermediate temperature and high temperature are given in Fig.5. It can be seen that there are two different deformation mechanisms under intermediate temperature, namely $\langle 110 \rangle$ {111} slip system moving in the matrix and

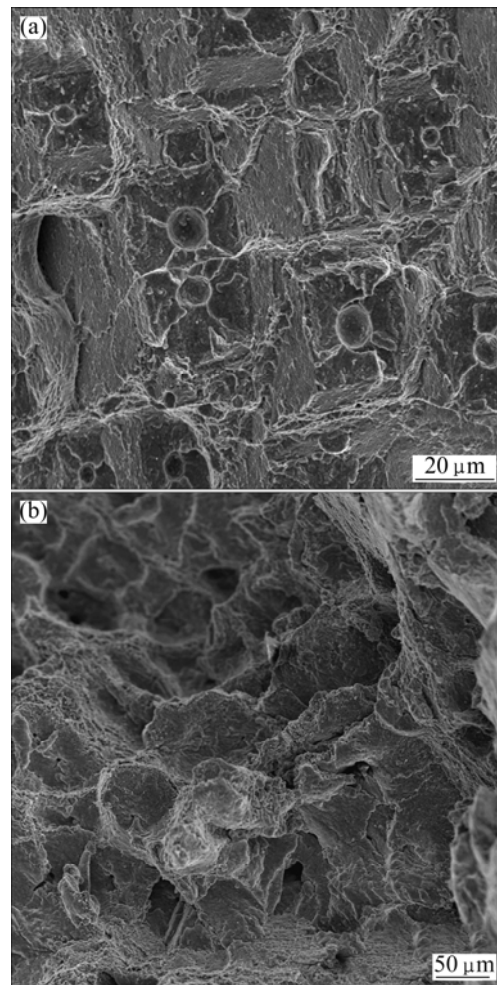


Fig. 4 Fracture morphologies of SRR99 alloys under typical creep conditions at intermediate temperature (a) and at high temperature (b)

$\langle 112 \rangle$ {111} dislocation shearing γ' -precipitates, as shown in Fig. 5(a). Plastic deformation starts from dislocations slipping in the matrix and then the primary creep is produced. With the progressive creep, transition from the primary creep to the secondary creep occurs when the activation of multiple slip systems leads to strong strain hardening and lower creep rates. Meanwhile, the shearing process involving $a/3\langle 112 \rangle$ dislocations is separated by superlattice intrinsic stacking faults (SISFs) or superlattice extrinsic stacking faults (SESFs), which plays an important role in the creep deformation. It is pointed out that the shearing of γ' -precipitates is the creep kinetics under such condition and therefore is the prevailing mechanism[12]. When this theory is used to explain the anisotropic stress–rupture behavior at intermediate temperature, nucleation and propagation of $a\langle 112 \rangle$ {111} dislocation are emphasized to be responsible for different stress–rupture properties between [001] and [011] orientations. Since it is easy to produce $a\langle 112 \rangle$ dislocation by dissociation of $\langle 110 \rangle$

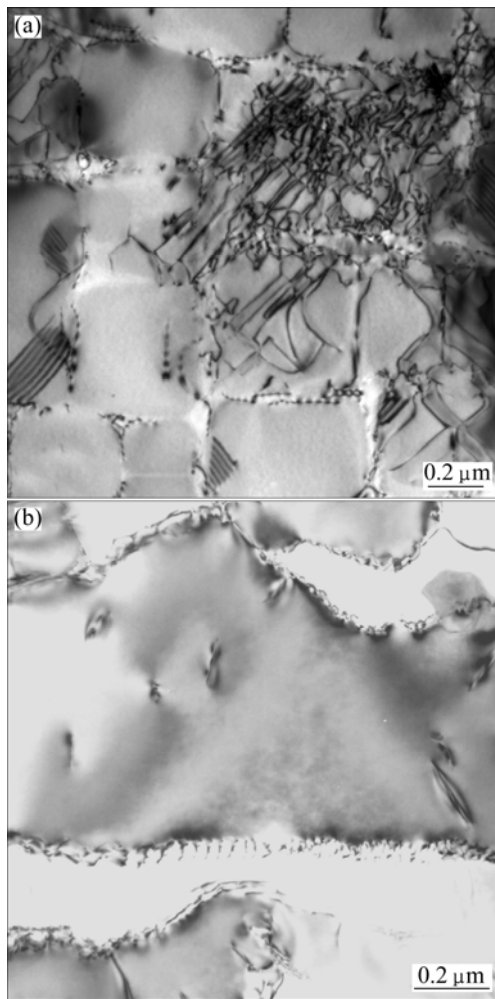


Fig. 5 TEM images of [001] SRR99 single crystal deformed at 760 °C, 700 MPa (a) and 900 °C, 350 MPa (b)

dislocation for single crystal with [011] orientation, thus, the shearing of γ' -precipitates by partial dislocations is more easy under a certain applied stress and decreases the stress–rupture life of [011]-oriented single crystal. As for single crystal near [111] orientation, poor stress–rupture property is related to co-planar slip of $\langle 110 \rangle \{111\}$ dislocations which reduce the probability of dislocation interaction and can not lead to work-hardening, as illustrated by CARON et al [13].

Taking the importance of [001]-oriented single crystals into account, special emphasis is placed on the effect of orientation deviation on stress–rupture property in detail. In fact, this can be rationalized in terms of a resolved shear stress on the primary $\alpha\langle 112 \rangle \{111\}$ slip system. Only if the stress exceeds a critical value which can activate $\alpha\langle 112 \rangle$ dislocation nucleation and propagation, can substantial primary creep occur. According to the method deduced by RAE and REED [14], a schematic contour plot is shown in Fig. 6 and the stress–rupture lives of some specimens are also denoted in the picture. The differences among the lives of these

specimens can be explained as follows: 1) the longer lives of specimens A, B and D are mainly due to near duplex slip boundary or multiple slip crystallographic orientation [001], which is easy to produce work-hardening and prolong stress–rupture life time; 2) the specimen C with shorter life compared with A, B and D is easy to nucleate $\alpha\langle 112 \rangle$ dislocations and promote γ' -cutting by superpartial dislocations when the critical shear stress is achieved; and 3) specimen F with the shortest life mainly results from the lowest critical resolved shear stress for $\alpha\langle 112 \rangle \{111\}$ dislocation propagation.

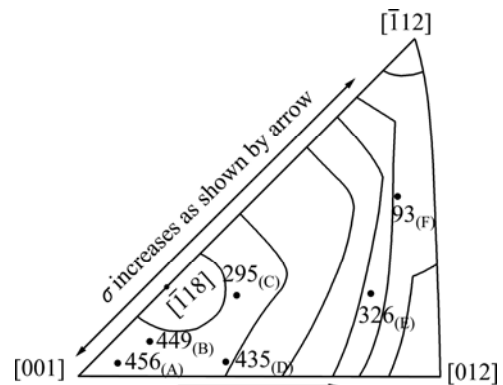


Fig. 6 Stress–rupture lifetime superimposed on stress threshold contour plot gained by REA and REED [14]

When the temperature is increased to about 900 °C, dislocation climb and cross-slip occur and they may dominate deformation mechanism, as shown in Fig. 5(b). On the other hand, shearing γ' -precipitates by $(a/2)\langle 110 \rangle$ dislocations coupled with a high-energy anti-phase boundary (APB) seems to substitute shearing mechanism forming stacking faults with increasing temperature. The reason to explain the temperature dependence of such transition is proposed according to the variation in APB energy or stacking fault energy (SFE) in Refs. [15–16]. Because the deformation mechanism is generally similar, the anisotropic creep behavior tends to disappear at higher temperature.

4 Conclusions

1) Single crystals with [001] orientation have the best stress–rupture property compared to those with [011] and [111] orientations, particularly at lower and intermediate temperatures.

2) The nucleation and propagation of $\alpha\langle 112 \rangle \{111\}$ slip system can be used to explain the influence of misorientation of crystal on the stress rupture properties of single crystals superalloys at lower and intermediate temperatures.

3) With increasing temperature, stress–rupture

properties of single crystals with three principal orientations tend to be equivalent. Dislocation climb and cross-slip dominate the deformation mechanism of single crystal superalloy.

References

- [1] REED R C. The superalloys: Fundamentals and applications [M]. New York: Cambridge University Press, 2006: 18–25.
- [2] BETTERIDGE W, SHAW S W S. Development of superalloys [J]. Mater Sci Technol, 1987, 3(13): 682–694.
- [3] MOTT N F, NABARRO F R N. Dislocation theory and transient creep [C]//Proceeding of bristol conference on the strength of solids. London: The Physical Society, 1948: 11–13.
- [4] JAX P, KRATOCHV P, HAASEN P. Solid solution hardening of gold and other FCC single crystals [J]. Acta Metall, 1970, 18(2): 237–245.
- [5] SASS V, GLATZEL U, FELLER-KNIEPMEIER M. Anisotropic creep properties of the nickel-base superalloy CMSX-4 [J]. Acta Mater, 1996, 44(5): 1967–1977.
- [6] BERTRAM A, OISCHEWSKI J. Anisotropic creep modelling of the single crystal superalloy SRR99 [J]. Comput Mater Sci, 1996, 5(1–3): 12–16.
- [7] GHOSH R N, CURTIS R V, MCLEAN M. Creep deformation of single crystal superalloys-modelling the crystallographic anisotropy [J]. Acta Metall Mater, 1990, 38(10): 1977–1992.
- [8] JIA Y X, JIN T, LIU J L, SUN X F, HU Z Q. Anisotropic creep in a Ni-based single crystal superalloy [J]. Acta Metallurgica Sinica, 2009, 45(11): 1364–1369.
- [9] MACKAY R A, MAIER R D. The influence of orientation on the stress rupture properties of nickel-base superalloy single crystals [J]. Metall Mater Trans A, 1982, 13(10): 1747–1754.
- [10] SASS V, SCHNEIDER W, MUGHRABI H. On the orientation dependence of the intermediate-temperature creep behaviour of a monocrystalline nickel-base superalloy [J]. Scripta Mater, 1994, 31(7): 885–890.
- [11] HAN G M, YU J J, SUN Y L, SUN X F, HU Z Q. Anisotropic stress rupture properties of the nickel-base single crystal superalloy SRR99 [J]. Mater Sci Eng A, 2010, 527(21–22): 5383–5390.
- [12] LEVERANT G R, KEAR B H. The mechanism of creep in gamma prime precipitation-hardened nickel-base alloys at intermediate temperatures [J]. Metall Trans, 1970, 1(2): 491–498.
- [13] CARON P, OHTA Y, NAKAGAWA Y G, KHAN T. Creep deformation anisotropy in single crystal superalloys [C]//DUHL D N. Proc Superalloys 1988. Warrendale PA: The Metallurgical Society, 1988: 215–224.
- [14] RAE C M F, REED R C. Primary creep in single crystal superalloys: Origins, mechanisms and effects [J]. Acta Mater, 2007, 55(3): 1067–1081.
- [15] DÉCAMP B, MORTON A J. On the mechanism of shear of γ' precipitates by single $(a/2)\langle 110 \rangle$ dissociated matrix dislocations in Ni-based superalloys [J]. Philos Mag A, 1991, 64(3): 641–668.
- [16] LEVERANT G R, KEAR B H. Creep of precipitation-hardened nickel-base alloy single crystals at high temperature [J]. Metall Trans, 1973, 4(1): 355–362.

温度对镍基单晶高温合金 SRR99 持久各向异性行为的影响

韩国明, 杨彦红, 于金江, 孙晓峰

中国科学院 金属研究所, 沈阳 110016

摘要: 为了揭示单晶高温合金 SRR99 在 650–1 040 °C 温度范围内及典型应力条件下的持久各向异性行为, 采用扫描电镜和透射电镜对持久实验后试样的断口形貌和微观组织演化进行研究。从 Larson-Miller 曲线看出, 在中低温条件下, [001]取向单晶具有最好的持久性能, 而[011]和[111]取向的持久性能相差不大; 随着温度的升高, 3 个主取向的持久性能的差异逐渐缩小, 到 1 040 °C 时几乎相同。通过断口形貌和组织观察, 分析[001]取向单晶持久性能较佳的原因, 同时探讨取向偏离度对[001]取向单晶持久性能的影响。

关键词: 单晶高温合金; 持久性能; 各向异性; 变形机制

(Edited by FANG Jing-hua)